Section A-Research paper

Diosgenin-encapsulated PLGA nanoparticles induce oxidative stress-mediated cell death in Ehrlich ascites carcinoma cells by inducing G2/M phase cell cycle arrest

Surya Kanta Dey[a], Tamanna Roy[a], Debjani Chatterjee[a], Sounik Manna[a], Dibyendu Giri [a], Angsuman Das Chaudhuri[a], Anirban Majumder[a], Ananya Pradhan[a], Sujata Maiti Choudhury[a]*

[a] Biochemistry, Molecular Endocrinology and Reproductive Physiology Laboratory, Department of Human Physiology, Vidyasagar University, Midnapore- 721 102, West Bengal, India.

***Corresponding author:**

Prof. Sujata Maiti Choudhury

Department of Human Physiology

Vidyasagar University

Midnapore- 721 102, West Bengal, India

E-mail: sujata_vu@mail.vidyasagar.ac.in,

sujata.vu2009@gmail.com,

Tel: +91 94 7444 4646.

Abstract

Cancer constitutes a large group of diseases and is a prime cause of death worldwide. Erhlich ascites carcinoma (EAC), an extemporaneous murine adenocarcinoma, is one of the well-recognized models in cancer research. Diosgenin (DGN) is a naturally occurring steroidal saponin from fenugreek and wild yam. Polymer nanoparticles have potential applications in biomedicine, but one of the important concerns is their safety. The present study aimed to evaluate the anti-cancer activity of diosgenin-encapsulated PLGA nanoparticles (PLGA-DGN NPs) against Ehrlich ascites carcinoma. The synthesized PLGA-DGN NPs were characterized by dynamic light scattering and surface zeta potential measurement, UV-vis spectroscopy, and Fourier transform infrared (FTIR) spectroscopy. The antineoplastic potency of PLGA-DGN NPs against EAC cells was assessed through cell viability assay, oxidative stress, chromatin condensation, and cell cycle arrest by flow cytometry. The cytotoxicity of PLGA-DGN NPs in EAC cells indicates the MTT assay revealed that high cytotoxic efficacy of PLGA-DGN NPs against EAC cells with the IC_{50} value of PLGA-DGN NPs was 7.91µg/ml. The oxidized glutathione (GSSG) increased compared to EAC control and decreased the level of reduced glutathione (GSH) in PLGA-DGN NPs, DGN rather than EAC control. In EAC cells, ROS formation was determined by H_2DCF_2DA staining using fluorescence microscopy showed PLGA-DGN NPs elevated the intracellular ROS generation at their respective IC_{50} doses

indicating potent apoptotic activity compared to DGN-treated EAC cells and EAC control. PLGA-DGN NPs exhibited cytotoxicity and induced apoptosis by increasing reactive oxygen species, chromatin condensation, cell cycle arrest at the G2/M phase, expression of pro-apoptotic proteins, and mitochondrial dysfunction in EAC. All the results indicate that PLGA-DGN NPs exert cytotoxic, oxidative stress, and apoptotic effect. In conclusion, the findings demonstrate that PLGA-DGN NPs may act as potential beneficial agents in carcinoma chemoprevention.
Keywords: Diosgenin, PLGA; EAC; Oxidative stress; Cell cycle arrest.

Introduction

One of the most common experimental tumors, Ehrlich ascites carcinoma (EAC), is crucial for modeling. It was used as an experimental tumor by Ehrlich and Apolant, in 1905[1], when it initially appeared as spontaneous breast cancer in a female mouse[2]. Tumour tissues were transplanted under the skin from one mouse to another. EAC, an undifferentiated carcinoma, is initially hyperdiploid, highly transplantable, non-regressive, rapidly increasing, brief in life span, and 100% malignant. According to a recent study, cisplatin co-treatment against Ehrlich ascites carcinoma resulted in substantial reductions in tumor cell number, viability, growth rate, and proliferative potential, as well as enhanced apoptosis and G0/G1 and sub-G1 cells cycle arrest[3]. The effectiveness of *in vivo* anti-proliferative therapy against EAC cells was also examined. Genestin showed a significant reduction in tumor weight, volume, high-mobility group box 1 (HMGB1), and nuclear factor-kappa B (NF-B) levels as compared to the control group[4]. The cancer chemotherapeutic strategies need to shift from discovery to novel cancer therapies to refining existing strategies and diagnostics in effective, advanced, and plausible ways[5].

Nanotechnology may be a possible solution by implementing it in cancer management. Nanotechnology offers novel therapeutic strategies with better targeting specificity, increased drug localization with high efficiency, reduced systemic toxicity, better improvement of diagnostic specificity, and improved imaging and radiation therapy[5]. The nanoparticles made by advanced nanotechnology is a promising contender in controlled drug delivery system (DDS)[6]. Nanocarrier-mediated drug delivery has been exploited to circumvent rapid degradation, low bioavailability, and inactivation of chemotherapeutic drugs[7]. In cancer nanotherapeutics, the application of polymeric nanoparticles (PNP) is gaining attraction due to its higher drug delivery efficiency, improved drug solubility, good pharmacokinetic profile, prolonged blood circulation time, and negligible side effects[8]. Polylactide-co-glycolide (PLGA) is an FDA-approved polymeric nanoparticle widely used for drug delivery for its biocompatibility, biodegradability, and non-toxic profile[9]. With the advent of nanomedicine, PLGA as a nanocarrier has found applications in various fields of medical research, such as biomechanics, chemotherapy, and immunology.

Phytochemicals, non-nutritive plant compounds with disease-protective or -preventive qualities, have been the subject of numerous investigations[10]. These substances are non-essential nutrients, meaning the human body does not need them to maintain life. Approximately 80% of

all breast cancer cases are ER (+). Tamoxifen and aromatase inhibitors are two examples of hormone treatments now used to treat ER (+) breast cancer[11]. Diosgenin (DGN) is a phytosterol saponin, mainly found in many plant species, including *Trigonella foenum-graecum* (fenugreek), *Heterosmilax species*, and *Dioscorea species*, particularly the roots of wild yam (*Dioscorea villosa*) [12]. About 137 types of Dioscorea species are considered the primary source of DGN; among them, 41 species contain more than 1% DGN[13]. A study by [14], proposed that DGN significantly inhibited the MCF-7 cell's proliferation by modulation of methylation status and microRNA-145 activation, but the migration capacity of MCF-7 cells was inhibited with a higher dose of DGN. Diosgenin was found to be a sensitive anti-cancer agent for triple-negative breast cancer cell line HCC1937 [15]. Inhibition of cell proliferation was observed in a dose and time-dependent manner after the treatment with DGN. Besides that, DGN induced apoptosis through the Bcl-2 associated X protein (Bax), caspase3 protein. Dioscin, an analog of DGN, induced apoptosis-mediated cell death by inhibiting pro-apoptotic proteins and inhibiting the invasion property of breast cancer cells by enhancing the GATA-binding protein 3 (GATA3)[16]. However, DGN is deprived of its clinical application due to its high hydrophobicity, poor bioavailability, and side effects.

Presents study aimed to synthesize non-toxic, biodegradable diosgenin-encapsulated PLGA nanoparticles (PLGA-DGN NPs) and evaluate it's *in vitro* anti-cancer potential against EAC cells.

Experimental

Materials and methods: Diosgenin (≥93%), Poly (D, L-lactic-co-glycolic) acid (PLGA) (lactic acid: glycolic acid 50:50) (Mw = 18,000), Dimethyl sulfoxide (DMSO), 3-(4,5-dimethyl-2-thiazolyl)-2,5-diphenyl-tetrazolium bromide (MTT), and F-68 (Poloxamer 188), penicillin and streptomycin were purchased from Sigma Aldrich Co, LLC, US. Propidium iodide, DAPI, and Fetal bovine serum (FBS) were procured from GIBCO. Merck provided all the chemicals and reagents used in the current investigation, which were all analytical quality.

Preparation of DGN-encapsulated PLGA nanoparticles

Diosgenin-encapsulated PLGA Nanoparticles (PLGA-DGN NPs) were formulated by the Nano precipitation technique described in our previous publication[9] with minor modifications. In brief, a weight amount of PLGA and DGN were co-dissolved in organic solvent acetone and vortexed for completely dissolved. Then an aqueous phage was prepared by taking 20 ml millipore water containing Pluronic F-68 solution (0.5%, w/v). Drop by drop, the organic phase was introduced to the aqueous phase while being stirred moderately magnetically overnight at room temperature. Acetone was completely evaporated, and the nanosuspension (MWCO: 12kDa) was then purified through dialysis. Then purified nanosuspension was centrifuged at 20,000 rpm at 4°C for 30 minutes, and the pellet was washed with PBS (pH 7.4) and, finally, lyophilized to obtain freeze-dried PLGA-DGN NPs. The entrapment efficiency (EE%) and loading capacity (LC%) were analyzed according to our previously reported methods[9].

Characterization

Dynamic light scattering (DLS) and electrophoretic light scattering (Laser Doppler, Malvern Instruments, U.K.) techniques were used to assess the size of PLGA-DGN NPs at 25°C at a 90° angle[17]. Zeta-sizer Nano ZS (ZEN 3600, Malvern Instruments, U.K.) was used to elaborate on the zeta potential measurements on the instrument equipped with a combination of Laser Doppler Velocimetry at 25°C. To assess the broadness of molecular weight distribution, The polydispersity index (PDI) PDI index is usually measured, and a larger PDI indicates broader molecular weight. The pH was fixed during the measurement in all samples. The entrapment efficiency (EE%) and loading capacity (LC%) were 78.68% and 8.38% respectively.

A UV-VIS-NIR spectrophotometer (UV-VIS-NIR spectrophotometer-3600, Shimadzu) was used to measure the PLGA-DGN NPs' absorption spectra. A 200-400 nm wavelength range was used to measure the absorbance spectra of DGN, VPLGA NPs, and PLGA-DGN NPs.

Fourier transforms infrared spectroscopy (FTIR) study of PLGA-DGN was carried out using an FTIR spectrophotometer (Perkin Elmer Spectrum Express Version 1.03.00), and the spectrum was recorded in the range of 4000–400 cm^{-1} with an accuracy of ±0.01 cm^{-1} and resolution of 4 cm^{-1}. Samples were mixed with potassium bromide (KBr) and compressed using a pressure of 200 kg/cm^2 for 2 min in a hydraulic press to make the pellets. FTIR spectra were observed using an FTIR spectroscope at the wavelength of 4000 to 400 cm^{-1} [9].

Cell culture and maintenance

The murine Ehrlich ascites carcinoma (EAC) cells were purchased from Chittaranjan National Cancer Institute, Kolkata, India. Cells were grown in a DMEM medium (GIBCO BRL, USA) containing 10% FBS (GIBCO BRL, USA) and antibiotics in appropriate conditions. Cell lines were cultured and maintained in Dulbecco's modified Eagle's medium (DMEM), supplemented with 10% fetal bovine serum (FBS), 2 mM L-glutamine, penicillin (100 units/mL) and streptomycin (100 µg/mL) under humidified atmosphere (95%) and 5% CO_2 at 37°C in a Co_2 incubator.

Anti-cancer activity

Cytotoxicity assay (MTT test)

A cell viability study was performed against EAC cells by 3-(4,5-dimethyl-2-thiazolyl)-2,5-diphenyl-tetrazolium bromide (MTT) assay[9]. Cells were seeded separately in 96-well plates at 1 × 106 cells/well density and grown for 72 hours. After cells reached 80% confluence, they were treated with different concentrations of free DGN and PLGA-DGN and incubated for 72 hours in a CO_2 incubator. To assess time-dependent cell viability, we assessed cell viability at different time points (24, 48, and 72 hours). At this predetermined time interval, freshly prepared MTT solution (5 mg\/mL) was added to each well, and the plate was incubated at 37°C for an additional 4 hours. During this incubation, formazan crystals formed and were solubilized by adding DMSO (0.1%) and mixed well by shaking the plate for 10 seconds. Absorbance was then measured at 540 nm using an ELISA analyzer (Bio-Rad, model 680). Experiments were performed in triplicate, and results are presented as mean ± SD standard deviation.

Study of Oxidative Stress

Measurement of Intracellular ROS generation

EAC cells were treated with DGN and PLGA-DGN NPs for 24 h at their respective IC_{50} doses. The next day, cells were washed with phosphate buffer, incubated with 1 µg/mL H_2DCFDA for 30 min at 37ºC, and rewashed thrice with culture media. Cells were found using a fluorescent microscope (LEICA DFC295 from Germany) and a fluorescence spectrophotometer (Hitachi F-7000) at 485 nm excitation and 520 nm emission, respectively. The experiment was done three times[17].

Measurement of reduced glutathione (GSH) and oxidized glutathione (GSSG)

Intracellular GSH AND GSSG were estimated by EAC cells with free DGN and PLGA-DGN NPs for 24 h at their respective IC_{50} doses. The next day, culture media was removed, and performed cell lysis by lysis buffer (0.1% Triton, 5 mM EDTA, 1 mM PMSF). The cell lysate was extracted, and sulfosalicylic acid (4%) was mixed with it, followed by centrifugation. Finally, GSH concentration was measured by DTNB assay[17]. To calculate the GSSG concentration, 2 µL of 2-vinyl pyridine was mixed with the samples and then performed DTNB assay.

Lactate dehydrogenase (LDH) release assay

EAC cells (1×10^6 cells/well) were treated with DGN and PLGA-DGN NPs for 24 h at their respective IC_{50} doses. The next day, culture media was removed, and a reaction mixture containing pyruvic acid, triton X-100, in PBS buffer (pH 7.4). Then 100 µL of reduced NADH (0.4 mg/mL) was added to the sample, and finally, the absorbance was taken at 340 nm by an ELISA microplate reader (Bio-Rad, Model 680)[18].

Study of chromatin condensation

Chromatin condensation was observed by DAPI and propidium iodide (PI) staining[17]. In brief, EAC cells (1×10^6 cells/well) were exposed to DGN and PLGA-DGN NPs for 24 hours at their corresponding IC50 concentrations. Cells that have not been treated are regarded as the control group. Then cells were washed with PBS (pH 7.4), 4% paraformaldehyde solution was used for cell fixation and then stained by DAPI (0.5 g/mL) and RNAse-PI (1mg ml^{-1}) for 15 min at 37°C. Finally, cells were washed twice with PBS, and images were taken by a fluorescence microscope (LEICA DFC295, Germany).

Cell cycle study

EAC cells (1×10^6 cells) were treated with DGN and PLGA-DGN at their respective IC_{50} doses for 24 h. After that, cells were washed thrice by centrifugation at 2000 rpm for 5 min, followed by fixation using 70% chilled ethanol. Then cells were again centrifuged for washing and treated with RNAse A (10 µL) at 37°C for 1 h. Then propidium iodide (25 µL) staining was performed in the dark at room temperature. After washing with PBS (pH 7.4), DNA content in the cell was analyzed by a flow cytometer (BD FACSVerse)[19].

Statistical analysis

All results were presented as mean ± standard deviation (S.D.) for all studies carried out in triplicate. One and two-way analysis of variance (ANOVA) was used to analyze the data's

statistical significance and multigroup comparisons. Then GraphPad Prism and Origins 8 (OriginLab, Northampton, USA) were used for the Tukey post hoc test. All Statistical significance was considered at $p < 0.05$.

Results and Discussion

The hydrodynamic diameters and size distribution of PLGA-DGN NPs were investigated utilizing the DLS technique. Results showed particle size 147.98 ± 3.45, and the size distributions were mono-dispersed. The ζ-Potential of the PLGA-DGN NPs exhibited negative values of 26 mV±0.62 (Table 1).

The UV-Vis and FTIR spectroscopic analysis was discussed in our previous paper (Dey et al., 2022). The report exposed that DGN showed a maximum absorbance peak at λ_{max}=210 nm, which was shifted to λ_{max} =213 nm after forming PLGA-DGN NPs. An increment of the polarity of PLGA-DGN NPs might cause this shifting.

FTIR spectra showed (Figure 1F) the characteristic bands of DGN at 3457 cm^{-1}, 2948 cm^{-1}, 2800-and 3600 $cm^{-1,}$ respectively, due to -OH, $-CH_2$, $-CH_3$ stretching vibration. PLGA-DGN NPs exhibited all these characteristic peaks at 3642 cm^{-1}, 3490 cm^{-1}, 2941 cm^{-1}, and 1759 cm^{-1}. Though some minor peaks shifting was noted due to hydrogen bonding, van der Waals' force, and dipole-dipole interaction[9].

Table 1. Characterization of PLGA-DGN NPs. Result is expressed as (mean ± S.D.; n = 3).

Formulation	Hydrodynamic Size (nm)	polydispersity index (PDI	Zeta potential (mV)	entrapment efficiency (EE%)	Loading capacity (LC%)
PLGA-DGN NPs	147.98±3.45	0.125±0.02	-28±0.52	78.68±6.13	8.38±1.84

Cytotoxic effect of PLGA-DGN NPs against EAC cells

Cell viability was examined in a concentration and time-dependent manner using the MTT assay. The results showed that PLGA-DGN NPs significantly inhibited EAC cell viability with increasing concentrations compared to DGN (Fig 1). The IC_{50} values were 7.91 µg/mL for DGN and 1.62 µg/mL for PLGA-DGN-NP. PLGA-DGN NPs also showed a significant decrease in cell viability at 48 and 72 hours, respectively. Cell viability studies revealed that PLGA-DGN NPs have significant cytotoxic potential compared to DGN[9].

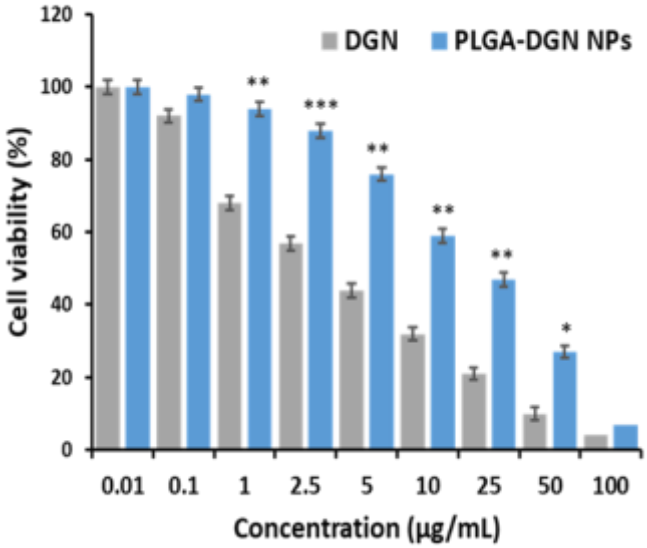

Fig 1. *In vitro* cell viability study in EAC cells after the treatment with DGN and PLGA-DGN NPs against at different concentrations (0.001 to 100 µg/mL) Results are expressed as (mean ± S.D; n=3; *p<0.05, **p<0.01, ***p<0.001)

Evaluation of oxidative stress

The potential of PLGA-DGN NPs to produce oxidative stress in EAC cells was evaluated by measuring free radicals and antioxidant activity. Results showed that after the treatment with PLGA-DGN NPs, the DCF intensity was significantly increased compared to free DGN. This DCF was formed from non-fluorescence H_2DCFDA by oxidation reaction in the presence of ROS and has given bright green fluorescence (Fig 2 & Fig 3). Besides that, PLGA-DGN NPs also induced the GSH to GSSG conversion. As shown in Fig 3, the GSH levels decreased significantly, and the GSSG level was increased in the PLGA-DGN NPs treated group compared to DGN. A significant increase in LDH level in EAC cells was also observed in PLGA-DGN NPs treated group compared to free DGN (Fig 3). Hence, these results confirmed that PLGA-DGN NPs produced oxidative stress in EAC cells by generating excessive ROS.

Study of nuclear morphology

Nuclear morphology was analyzed by evaluating chromatin condensation in EAC cells. Cells were stained with DAPI and PI to study chromatin condensation. Fig 2 presented shrunken and irregular nuclear morphology with red spherical beads in DAPI and PI-stained cells in the PLGA-DGN NPs treated group. However, no notable change was visualized in DGN-treated groups.

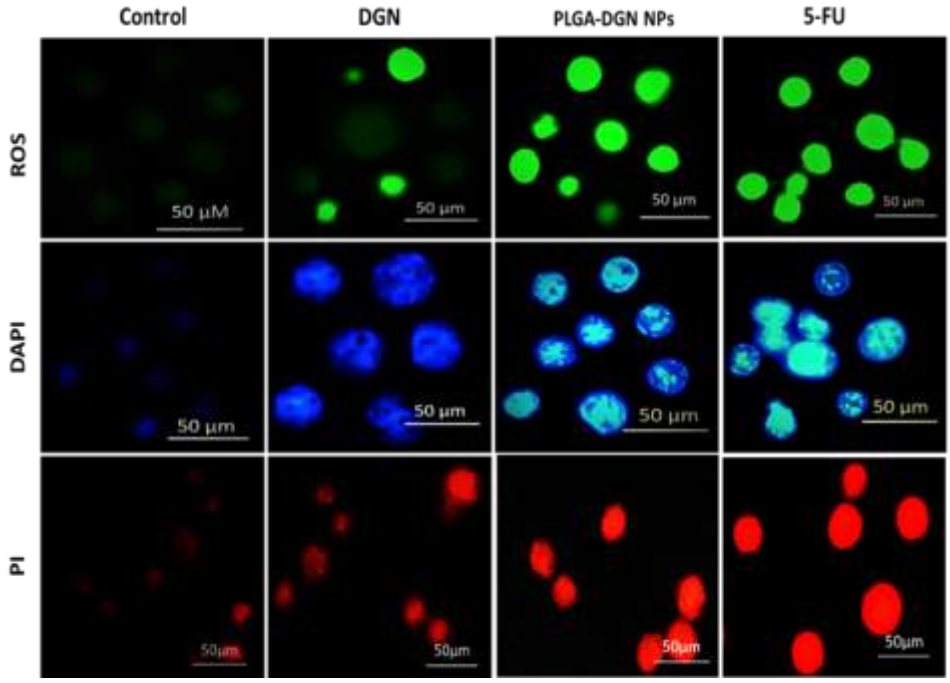

Fig 2. Study of ROS generation and chromatin condensation in EAC cells after the treatment with DGN, PLGA-DGN NPs. Fluorescence microscopic observation of intracellular ROS generation by H2DCFDA staining, nuclear morphology by DAPI, and PI staining. Scale bar: 50 µm

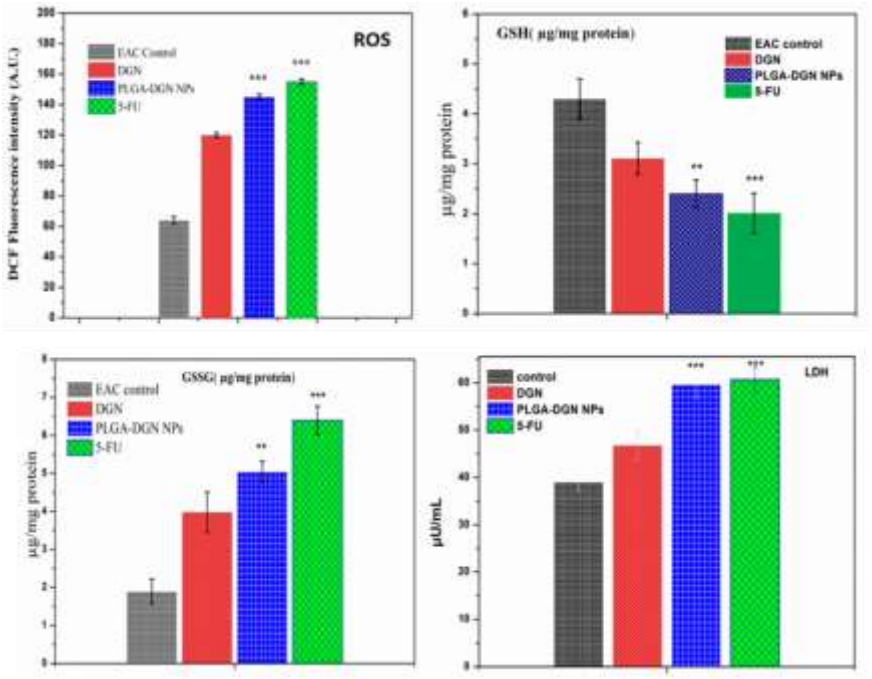

Fig 3. Measurement of DCF fluorescence intensity in ROS generation by spectrofluorometer; Measurement of reduced glutathione (GSH), oxidized glutathione (GSSG) and Lactate dehydrogenase (LDH). Results are expressed as (mean ± S.D; n=3; *p<0.05, **p<0.01, ***p<0.001)

Evaluation of cell cycle arrest

The proportion of the cell population in the G2/M phage of the cell cycle was considerably higher in the PLGA-DGN NPs treated group, according to the flow cytometry analysis of the cell cycle. Whereas no significant cell cycle change was observed in the DGN-treated group. So, PLGA-DGN NPs induced cell cycle arrest at the G2/M phage (Fig 4).

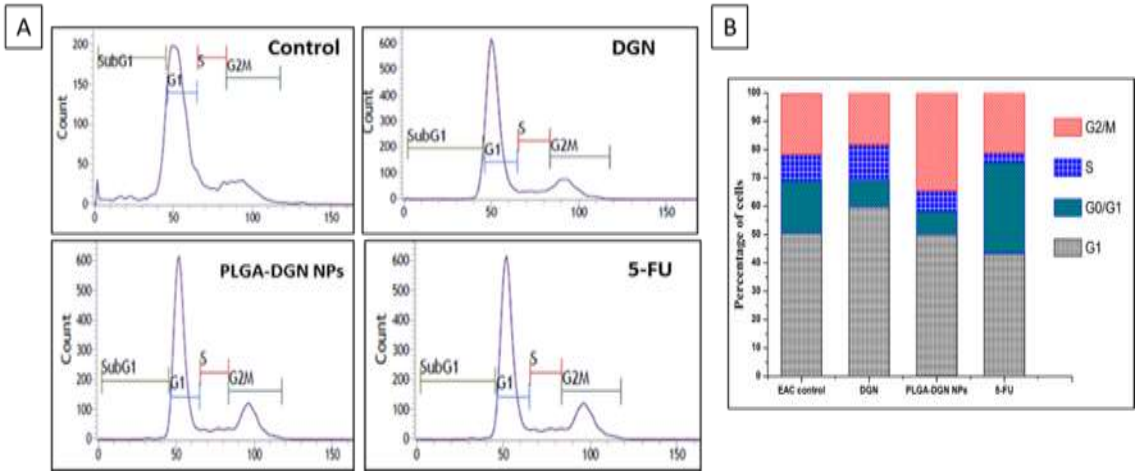

Fig 4. Flow cytometry analysis of cell cycle. Figure shows the percentage of cells at different pages of the cell cycle (A-B).

Conclusion

In this investigation, we successfully prepared and characterized biodegradable, biocompatible, and non-toxic PLGA-DGN NPs with desirable sizes with narrow distribution and high loading capacity. We epitomized the hypothesis that PLGA-DGN NPs stimulate ROS generation and produce oxidative stress, which induces chromatin condensation. Simultaneously, PLGA-DGN NPs induced cell cycle arrest at G2/M phage, exerting a cytotoxic effect through oxidative stress-mediated cell death.

Acknowledgments

The University Science Instrumentation Centre (USIC), Vidyasagar University, Midnapore, and West Bengal, India, thank the authors for providing the resources needed to carry out these experiments. The Indian Institute of Technology in Kharagpur, the Chittaranjan National Cancer Institute in Kolkata, and the Bose Institute in Kolkata provided the writers with helpful facilities. We are also grateful to Dr. Ashok Maiti, MD Pathologist, Medipath Diagnostic and Consultation Centre, Midnapore, Paschim Medinipur, West Bengal for giving us healthy human blood samples.

Disclosure statement

All authors declare that they have no conflict of interest.

Funding

No

Abbreviation

EAC-Ehrlich ascites carcinoma cells
DGN-Diosgenin
PLGA- Poly (D, L-lactic-co-glycolic) acid
PLGA-DGN NPs- Diosgenin encapsulated Poly (D, L-lactic-co-glycolic) acid nanoparticles
PBS- Phosphate buffered saline
ABS- Acetate buffered saline
EE-Entrapment efficiency
LC-Loading capacity
ROS-Reactive oxygen species
GSH-Reduced glutathione
GSSG-Oxidized glutathione
LDH-Lactate dehydrogenase

References

1.Ehrlich, P., Apolant, H. (1905). Beobachtungen Über Maligne Mausentumoren. Berlin. Klin. Wschr. 28,871-874.

2. Saleh, N., Allam, T., Abdelfattah, A., & El-Borai, N. (2022). Review on Ehrlich Ascites Carcinoma in Mice and Cancer Treatment with Special Reference to The Potential Protective and Therapeutic Effects of Hesperidin Versus Cisplatin. Journal of Current Veterinary Research, 4(1), 47-57.

3. Morsi, D. S., Barnawi, I. O., Ibrahim, H. M., El-Morsy, A. M., El Hassab, M. A., & Abd El Latif, H. M. (2023). Immunomodulatory, apoptotic and anti-proliferative potentials of sildenafil in Ehrlich ascites carcinoma murine model: *In vivo* and in silico insights. International Immunopharmacology, 119, 110135.

4. Saleh, M. A., Antar, S. A., Abdo, W., Ashour, A., & Zaki, A. A. (2023). Genistin modulates high-mobility group box protein 1 (HMGB1) and nuclear factor kappa-B (NF-κB) in Ehrlich-ascites-carcinoma-bearing mice. Environmental Science and Pollution Research, 30(1), 966-978.

5. Kemp, J. A., & Kwon, Y. J. (2021). Cancer nanotechnology: current status and perspectives. Nano convergence, 8(1), 34.

6. Dang, Y., & Guan, J. (2020). Nanoparticle-based drug delivery systems for cancer therapy. Smart Materials in Medicine, 1, 10-19.

7. Edis, Z., Wang, J., Waqas, M. K., Ijaz, M., & Ijaz, M. (2021). Nanocarriers-Mediated Drug Delivery Systems for Anti-cancer Agents: An Overview and Perspectives. International journal of nanomedicine, 16, 1313–1330.

8. Yousefi Rizi, H. A., Hoon Shin, D., & Yousefi Rizi, S. (2022). Polymeric Nanoparticles in Cancer Chemotherapy: A Narrative Review. Iranian journal of public health, 51(2), 226–239.

9. Dey, S. K., Pradhan, A., Roy, T., Das, S., Chattopadhyay, D., & Choudhury, S. M. (2022). Biogenic polymer-encapsulated diosgenin nanoparticles: Biodistribution, pharmacokinetics,

cellular internalization, and anti-cancer potential in breast cancer cells and tumor xenograft. Journal of Drug Delivery Science and Technology, 76, 103743.

10. Pires, T. C. D. S. P. (2020). Development of new food products of high nutritional and functional value using flowers, fruits and plant stems.

11. Toss, A., Tomasello, C., Razzaboni, E., Contu, G., Grandi, G., Cagnacci, A., ... & Cortesi, L. (2015). Hereditary ovarian cancer: not only BRCA 1 and 2 genes. BioMed research international, 2015.

12. Raju, J., Patlolla, J. M., Swamy, M. V., & Rao, C. V. (2004). Diosgenin, a steroid saponin of Trigonella foenum graecum (Fenugreek), inhibits azoxymethane-induced aberrant crypt foci formation in F344 rats and induces apoptosis in HT-29 human colon cancer cells. Cancer epidemiology, biomarkers & prevention: a publication of the American Association for Cancer Research, cosponsored by the American Society of Preventive Oncology, 13(8), 1392–1398.

13. Jesus, M., Martins, A. P., Gallardo, E., & Silvestre, S. (2016). Diosgenin: Recent Highlights on Pharmacology and Analytical Methodology. Journal of analytical methods in chemistry, 2016, 4156293.

14. Li, J., Liu, X., Guo, M., Liu, Y., Liu, S., & Yao, S. (2005). Electrochemical study of breast cancer cells MCF-7 and its application in evaluating the effect of diosgenin. *Analytical sciences*, *21*(5), 561-564.

15. Huang, N., Yu, D., Wu, J., & Du, X. (2021). Diosgenin: an important natural pharmaceutical active ingredient. Food Science and Technology, 42.

16. Aumsuwan, P., Khan, S. I., Khan, I. A., Walker, L. A., & Dasmahapatra, A. K. (2016). Gene expression profiling and pathway analysis data in MCF-7 and MDA-MB-231 human breast cancer cell lines treated with dioscin. Data in brief, 8, 272-279.

17. Pradhan, A., Bepari, M., Maity, P., Roy, S. S., Roy, S., & Choudhury, S. M. (2016). Gold nanoparticles from indole-3-carbinol exhibit cytotoxic, genotoxic and antineoplastic effects through the induction of apoptosis. RSC advances, 6(61), 56435-56449.

19.Fatemizadeh M, Tafvizi F, Shamsi F, Amiri S, Farajzadeh A, Akbarzadeh I. Apoptosis induction, cell cycle arrest and anti-cancer potential of tamoxifen-curcumin loaded niosomes against MCF-7 cancer cells. Iranian Journal of Pathology. 2022;17(2):183.

20. Roy, T., Dey, S. K., Pradhan, A., Chaudhuri, A. D., Dolai, M., Mandal, S. M., & Choudhury, S. M. (2022). Facile and Green Fabrication of Highly Competent Surface-Modified Chlorogenic Acid Silver Nanoparticles: Characterization and Antioxidant and Cancer Chemopreventive Potential. ACS omega.

Author affiliations

Corresponding Author:

Sujata Maiti Choudhury[a]*

Biochemistry, Molecular Endocrinology and Reproductive Physiology Laboratory, Department of Human Physiology, Vidyasagar University,

Midnapore 721 102, West Bengal, India;
orcid.org/0000-0002-5239-1352
E-mail: sujata_vu@mail.vidyasagar.ac.in, sujata.vu2009@gmail.com

Authors

Surya Kanta Dey[a]
Biochemistry, Molecular Endocrinology and Reproductive Physiology Laboratory, Department of Human Physiology, Vidyasagar University, Midnapore- 721 102, West Bengal, India.
E-mail:suryakantadey6@gmail.com

Tamanna Roy[a]
Biochemistry, Molecular Endocrinology and Reproductive Physiology Laboratory, Department of Human Physiology, Vidyasagar University, Midnapore- 721 102, West Bengal, India.
E-mail:tamanna.micro@gmail.com

Debjani Chatterjee[a]
Biochemistry, Molecular Endocrinology and Reproductive Physiology Laboratory, Department of Human Physiology, Vidyasagar University, Midnapore- 721 102, West Bengal, India.
E-mail: dchatterjee.mid@gmail.com

Sounik Manna[a]
Biochemistry, Molecular Endocrinology and Reproductive Physiology Laboratory, Department of Human Physiology, Vidyasagar University, Midnapore- 721 102, West Bengal, India.
E-mail:sounikmanna94@gmail.com

Dibyendu Giri [a]
Biochemistry, Molecular Endocrinology and Reproductive Physiology Laboratory, Department of Human Physiology, Vidyasagar University, Midnapore- 721 102, West Bengal, India.
E-mail: giridibyendu60@gmail.com

Angsuman Das Chaudhuri[a]
Biochemistry, Molecular Endocrinology and Reproductive Physiology Laboratory, Department of Human Physiology, Vidyasagar University, Midnapore- 721 102, West Bengal, India.
E-mail: angsubabai@gmail.com

Anirban Majumder[a]
Biochemistry, Molecular Endocrinology and Reproductive Physiology Laboratory, Department of Human Physiology, Vidyasagar University, Midnapore- 721 102, West Bengal, India.
E-mail: anirbanmajumder2005@gmail.com

Ananya Pradhan[a]
Biochemistry, Molecular Endocrinology and Reproductive Physiology Laboratory, Department of Human Physiology, Vidyasagar University, Midnapore- 721 102, West Bengal, India.
E-mail: ananyapradhan84@gmail.com